

Accumulation and Discharge of Pore Pressure under Cyclic Loading in Light-Duty Road Pavement Structures

Accumulation et décharge de la pression interstitielle sous chargement cyclique dans des structures de chaussées routières légères

K. Koivisto

Ramboll Finland Oy, Espoo, Finland

L. Korkiala-Tanttu

Aalto University, Espoo, Finland

ABSTRACT: Low-volume roads are a notable part of the Finnish road network and the portion of public low-volume roads of the whole road network is high. Typical characteristics for low-volume roads are narrow shoulder areas as well as relative steep side slopes. The low-volume roads typically suffer from frost heave and insufficient drainage that result in permanent deformations (rutting) on the roads. Moisture is a main cause of deterioration in pavement sections and according to earlier studies, excess moisture in them can decrease the pavement life by more than half. In the early 2000s, accelerated pavement tests were done in Finland using typical low-volume road structure with side slopes of different steepness. In this paper we analyse the results of these measurements, with the aim to use them as the foundation in numerical modelling of the effect of increasing pore pressures on low-volume roads due to the increase of heavy vehicle traffic.

RÉSUMÉ: Les routes à faible volume constituent une partie notable du réseau routier finlandais et la part des routes publiques à faible volume de l'ensemble du réseau routier est élevée. Les caractéristiques typiques des routes à faible volume sont les zones de bas-côté et les pentes relativement abruptes. Les routes à faible volume souffrent généralement de soulèvement dû au gel et à un drainage insuffisant qui entraîne des déformations permanentes (ornières) sur les routes. L'humidité est l'une des principales causes de détérioration des sections de chaussée et, selon des études antérieures, une humidité excessive pourrait réduire de plus de moitié la durée de vie de la chaussée. Au début des années 2000, des essais accélérés de la chaussée ont été effectués en Finlande sur une structure routière typique à faible volume avec des pentes latérales de pentes différentes. Dans cet article, nous analysons les résultats de ces mesures dans le but de les utiliser comme base de la modélisation numérique de l'effet de l'augmentation de la pression interstitielle sur les routes à faible volume en raison de l'augmentation du trafic de véhicules lourds.

Keywords: pavement, pore pressure, cyclic loadig

1 INTRODUCTION

The amount of public low-volume roads in Finland is considerable and they form an important part

of the Finnish road network, due to the country being relatively large with comparatively small population. Typical characteristics for low-

volume roads are narrow shoulder areas and fairly steep side slopes.

Low-traffic pavements are subjected to variable hydraulic and mechanical loadings that have a strong influence on their behaviour, and a full modelling of these various coupled aspects has never as yet been achieved (Ho & al. 2014).

The research this paper is part of was launched because of a legislation change on 1.10.2013, according to which lorries with 4 or 5 axles and vehicle combinations with 8 or 9 axles must be increased. The effect of the change on road conditions needed to be studied, as heavy traffic is the main cause for damages in road structure, especially on the low-volume roads.

This article analyses the pore pressure results Korkiala-Tanttu et al. (2003) measured during accelerated pavement tests with light-duty road pavement structures that were implemented by VTT Technical Research Centre of Finland during 2002 with a heavy vehicle simulator (HVS).

The aim is to use these pore pressure measurements as the foundation in numerical modelling of the effect of increasing pore pressures on low-volume roads due to the increase of heavy vehicle traffic.

2 EFFECT OF WATER IN THE PAVEMENT STRUCTURE

Moisture is the main cause of deterioration in pavement sections (Cedergren 1994). Excess moisture in pavement sections can decrease the pavement life by more than half (Christopher and McGuffey 1997). Damage caused by moisture includes separating asphalt from aggregates (stripping), water bleeding and pumping, shrinking, swelling, and frost heave of the subgrade layer. Moisture can enter the pavement section through rainfall or by upward water flow caused by capillary forces.

In tests made by Saevarsdottir & Erlingsson (2013) water had a significant effect on the structure, softening it and increasing the

accumulation of permanent deformation. There are several other factors that affect the resilient response and accumulation of permanent deformation of granular materials.

In northern climates, the stability of mechanical properties throughout the annual cycle has been proven to vary significantly. This is a notable issue, since pavement materials may reach high degree of saturation in northern conditions during spring thaw or otherwise through surface or subhorizontal water infiltration. (Bilodeau & Dore 2012)

3 VTT TEST STRUCTURES AND INSTRUMENTATION

3.1 Test structures

The test structure was built in a concrete basin with thermally insulated walls and a groundwater table regulation capacity. The total length of the basin was 36 m, with the depth of 2.5 m and width of 4 m at the top and 3 m at the bottom (Figure 1). There is a 3 x 3 m part of the test basin which is 4.5 m deep. (Korkiala-Tanttu et al. 2003)

The basin was split into three test sections (1, 2 and 3). Test sections 2 and 3 were built with two different side slopes and test section 1 without a slope. Side slope inclinations were 1:3 and 1:1,5. Soil materials and top layers were similar in the different sections (Figure 2). The length of each test section was eight meters. Two types of geotextiles were placed on the top of the clay, a bi-component geotextile (BCG) at the outside ends of test sections 1 and 3 and a traditional geotextile between the bi-component geotextiles. During the test the pass of the HVS wheel load was identical on each of the areas. (Korkiala-Tanttu et al. 2002)

All the test sections consisted of a thin asphalt surfacing of 50 mm, a 400 mm base layer of crushed rock and a 200 mm subbase layer of gravel. (Korkiala-Tanttu et al. 2002)

3.2 Instrumentation

In test sections 1 and 3 there were two pore pressure cells in the clay layer at both test

sections. One was situated under the BCG and the other in the reference area beneath the traditional geotextile. In test section 2 there was one pore pressure cell in the clay layer. The heads of pore pressure cells were on the level +15.64 some 100 mm under the geotextile. The pressures were recorded first once an hour and later on once per half an hour. (Korkiala-Tanttu et al. 2003)

3.3 The testing procedure

Before the load testing, the groundwater level was elevated to the gravel surface (W2). The groundwater was kept at this level two weeks. After this, the water level was lowered to the upper part of the clay subgrade (W1). (Korkiala-Tanttu et al. 2002)

Test parameters and environmental conditions, including the water table regulation, were controlled during the HVS test. All sections were tested identically. At the beginning of test, the

water table was 50 mm under the clay surface (W1). At the end of test the water table was elevated to the top of the gravel layer during the test (W2) and to the centre of crushed rock (W3). Static and cumulative pore pressures were monitored with transducers. (Korkiala-Tanttu et al. 2002)

4 RESULTS FROM THE PORE PRESSURE MEASUREMENTS

4.1 The effect of time on pore pressure results outside of loading periods

The level of pore pressures measured in between the different test sections' loading periods was examined because large differences in the pore pressures existed in the measurements of different test sections during the loadings.

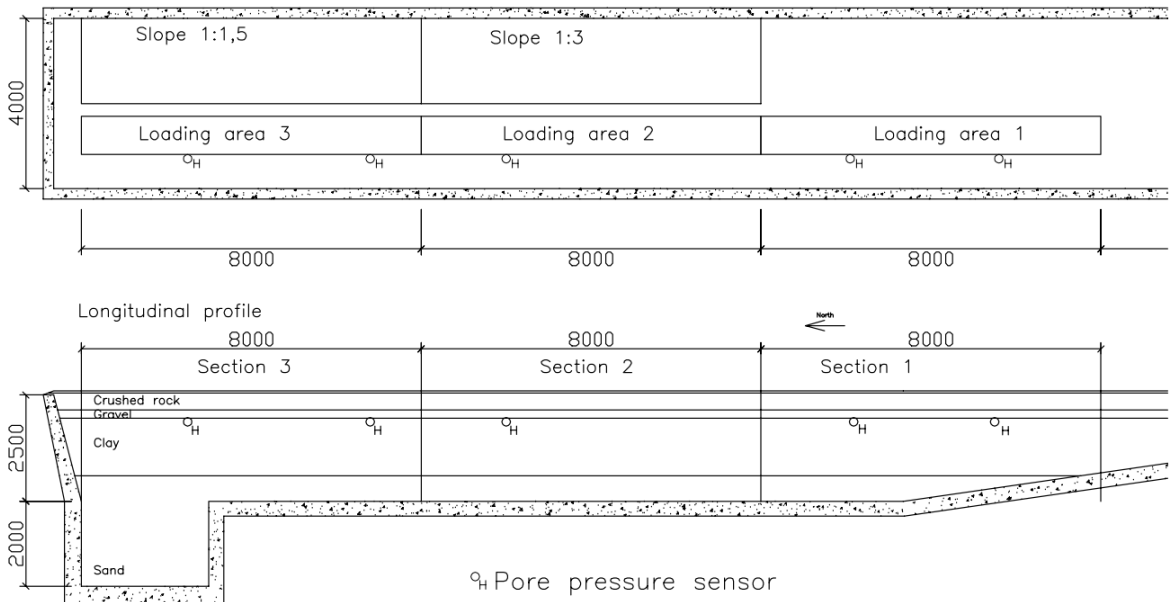


Figure 1. Plan and profile of the Otaniemi test basin and locations of pore pressure sensors in the HVS-tests for low-volume roads.

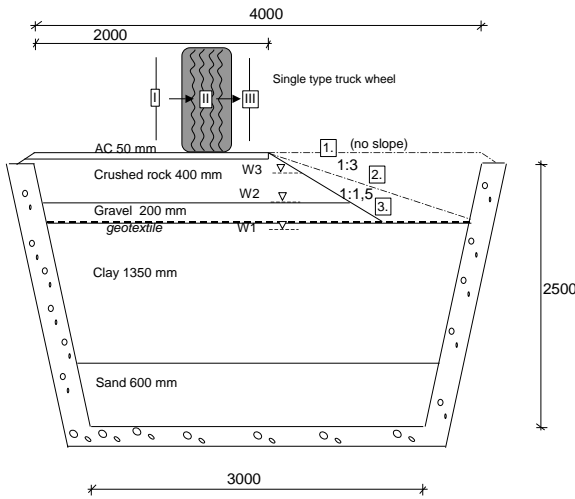


Figure 2. Cross section of low-volume road structures in Otaniemi test basin (Korkiala-Tanttu et al. 2002).

Figure 3 shows the measured pore pressures in different pressure cells before loading of the test section 1. Figure 4 presents the same results between loadings of test sections 1 and 2, and Figure 5 respectively between loadings of test sections 2 and 3. The results indicate that the overall level of pore pressure in the structures decreases in time and after each loading period the level drops lower than it was before the previous loading period. It can be presumed that

the pore pressure has still been elevated from the original change in the water level in earlier loading periods.

Due to the phenomenon described here, the absolute pore pressures between different loading periods cannot directly be compared with any confidence. A more reliable approach is to compare the changes in pore pressure between different loading periods.

4.2 The measurements of pore pressure due to loading in test section I

The test section 1 was built without slope and there were two pore pressure cells in the clay layer. Sensor 4 was situated in the reference structure, whereas sensor 3 was under the bi-component geotextile. The measurement results are shown in Figure 6.

The pore pressure curve of sensor 4 did not give proper response to the loading sequences. Comparing to the results from the other pore pressure sensors lead to the conclusion that the results from sensor 4 were undependable. This is most probably due to problems during installation of the sensor 4, where its final installation angle was 0° , whereas all the other sensors were installed in an angle of $52\dots54^\circ$.

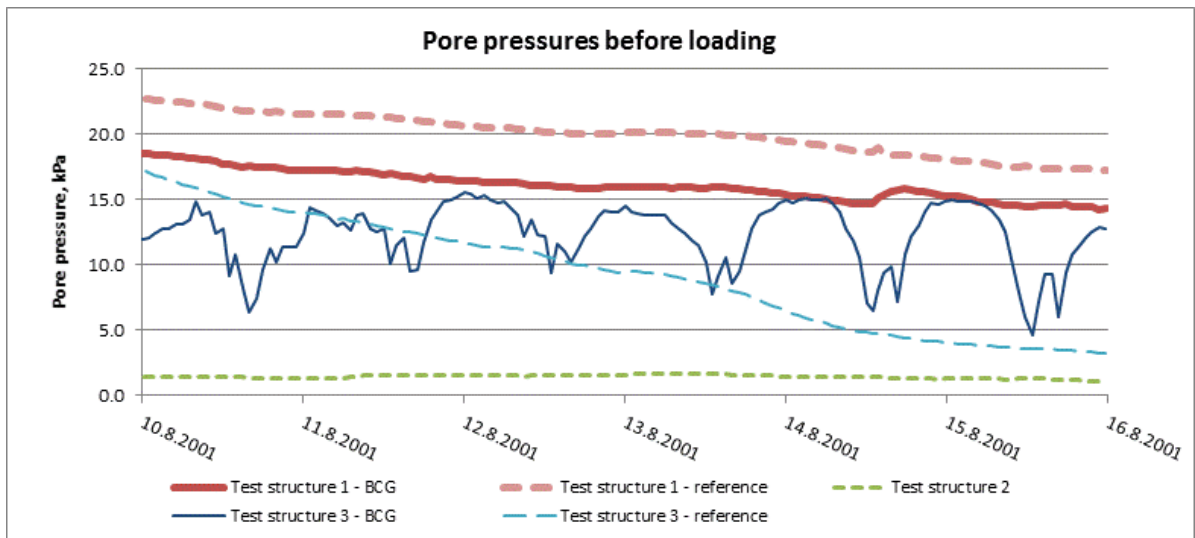


Figure 3. Measured pore pressure in the pore pressure cells before the loading.

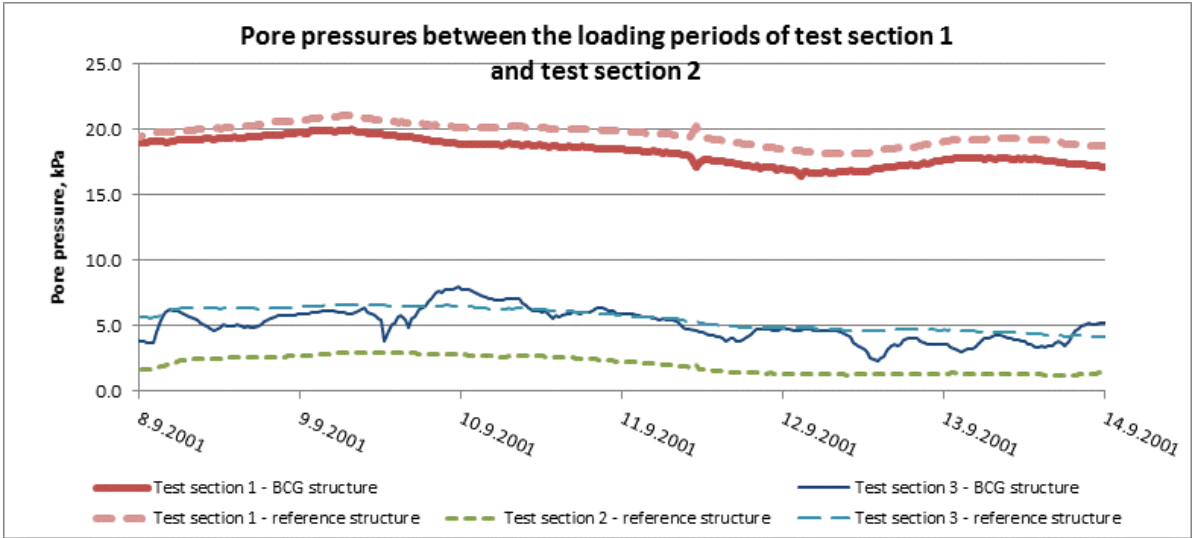


Figure 4. Measured pore pressure in the pore pressure cells between the loading periods of test section 1 and test section 2.

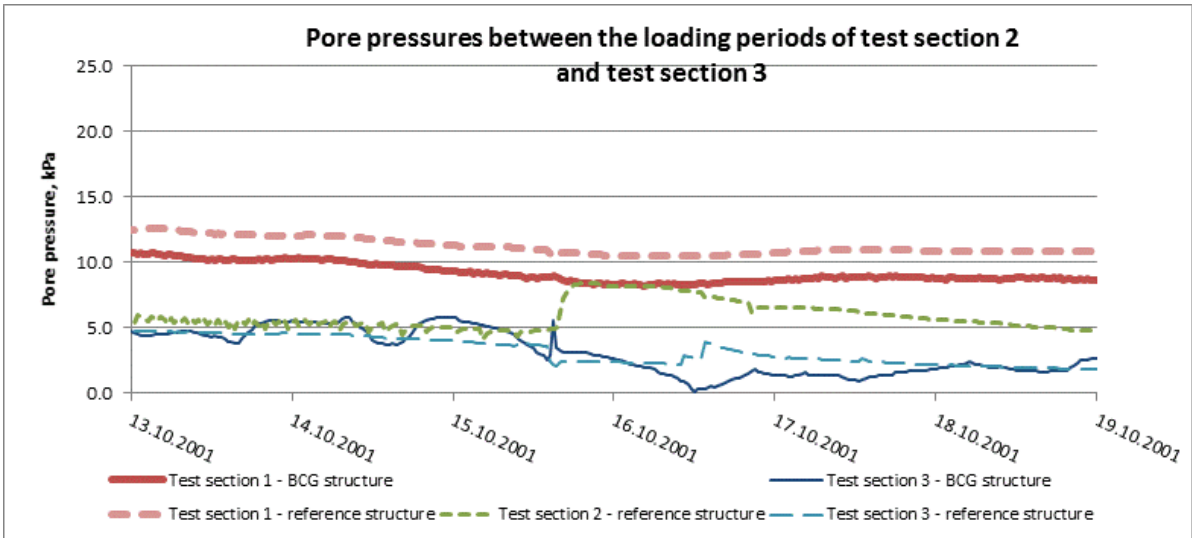


Figure 5. Measured pore pressure in the pore pressure cells between the loading periods of test section 2 and test section 3.

In the bi-component geotextile structure (BSG) the increase in pore pressure in sensor 3 is clear after each loading. The drop of pore pressure from the maximum value back to the initial level is very slow and gradual. Because of this, the second loading at 50 kPa happened

before pore pressure from the previous loading had dissipated.

Rising water level from W1 to level W2 caused an increase of approximately 2 kPa in the initial pore pressure level. Otherwise, no significant differences in pore pressure responses

can be observed during loading at water levels W1 and W2.

The maximum change in pore pressure in the BSG structure was 1...1,5 kPa with 30 kPa loading, approximately 1,2 kPa with 40 kPa loading and 2,2...3 kPa with 50 kPa loading respectively. With 30 kPa loadings the pore pressure was always fully dissipated before the next loading, whereas after 40 and 50 kPa loadings accumulation in the maximum pore pressure can be observed in Figure 6.

4.3 The measurements of pore pressure due to loading in test section 2

The test section 2 was built with conventional geotextile, with a slope that had an inclination of 1:3. There was one pore pressure cell in the clay layer (sensor 5). Figure 7 shows the measurement results from the section.

The increase in pore pressure after loading is clear. However, unlike in test section 1 with the

BSG structure, the level of pore pressure after loading drops very fast close to the initial level in 0,5...2 hours. After the immediate drop the dissipation is gradual, taking approximately 2 days.

The difference in initial pore pressures between water levels W1 and W2 is approximately 3 kPa and between water levels W2 and W3 approximately 1 kPa. However, this is not conclusive, since the pore pressures may not yet be fully developed when loading at water level W3 is started.

The dissipation of pore pressure after the last load sequence at water level W3 is very uneven compared to the dissipation after all the other loading sequences. Reason for this is unclear.

In test section 2 the maximum change in pore pressure is 4...11 kPa with 30 kPa loading, 4...5 kPa with 40 kPa loading and 4...20 kPa with 50 kPa loading respectively.

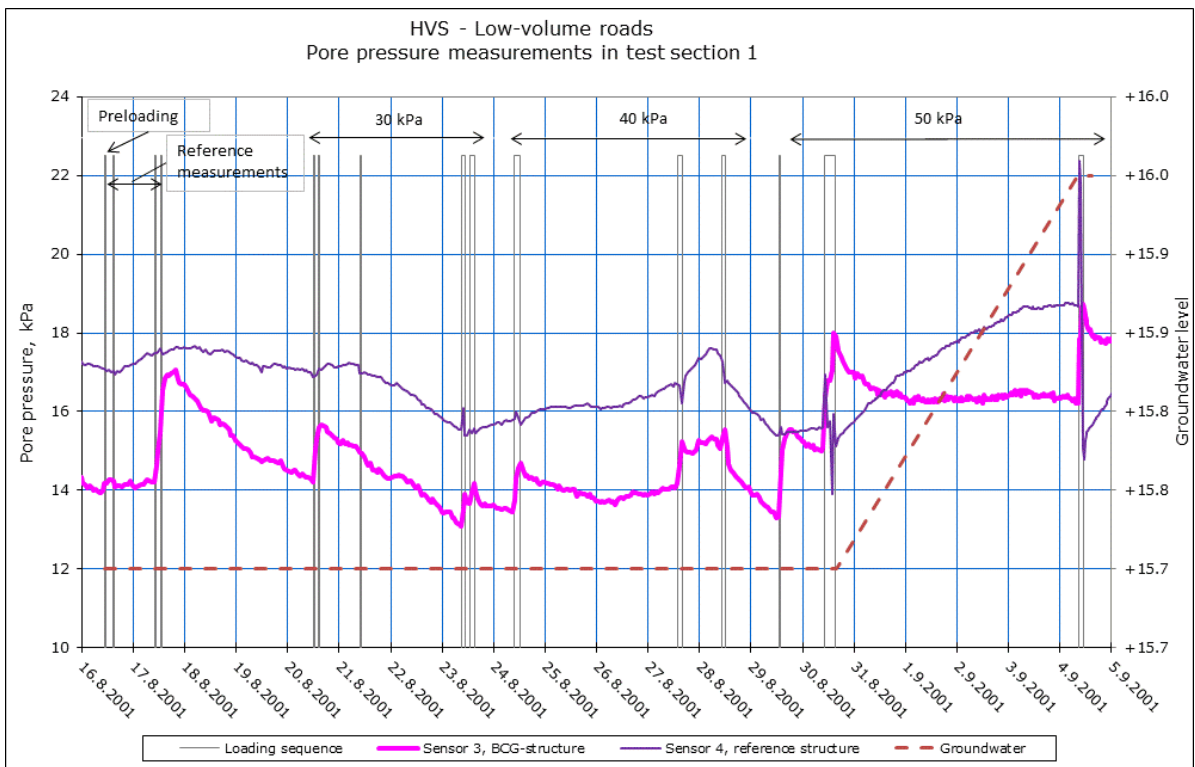


Figure 6. Measured pore pressures in test section 1 with 30, 40 and 50 kPa load sequences.

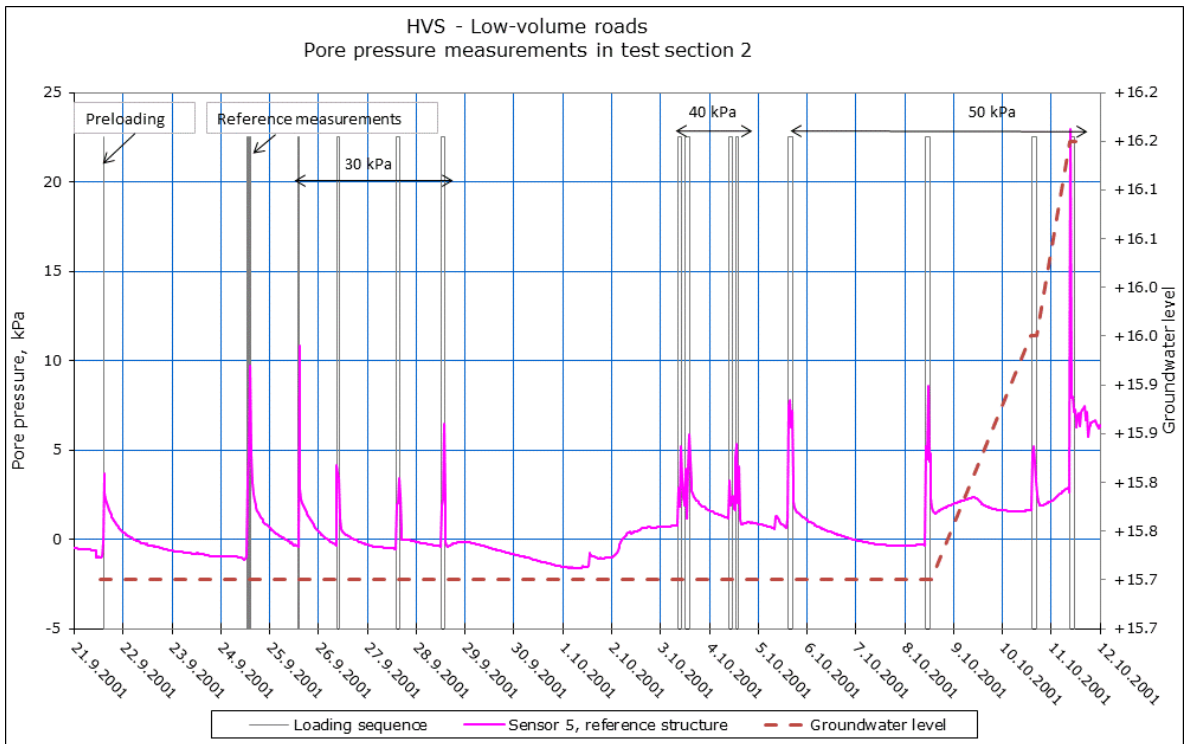


Figure 7. Measured pore pressures in test section 2 with 30, 40 and 50 kPa load sequences.

4.4 The measurements of pore pressure due to loading in test section 3

The test section 3 was built with slope 1:1,5 and there were two pore pressure cells in the clay layer. Sensor 1 was situated in the reference structure, whereas sensor 6 was under the bi-component geotextile. The measurement results are shown in Figure 8.

In test section 3 the increase in pore pressure after loading is clear. As with test section 2 with the BSG structure, the level of pore pressure after loading drops very fast to the initial level in 0,5...2 hours. After the immediate drop there is no remarkable dissipation to be seen later.

The difference in initial pore pressure between water levels W1 and W2 is approximately 2...3 kPa and between water levels W2 and W3 approximately 1 kPa. However, as is also the case with test section 2, this is not conclusive, since the pore pressure may not yet be fully developed when loading at water level W3 is started.

In test section 3 the maximum change in pore pressure is 9...18 kPa with 30 kPa loading, 8...33 kPa with 40 kPa loading and 8...70 kPa with 50 kPa loading respectively.

5 CONCLUSIONS

There were notable differences in the pore pressure levels of the different test sections especially before any loading had started. This is most likely due there having been not enough time for the pore pressures to set after the elevation of the ground water level. Some difference may have been caused by perceived leakage from the test basin during the test.

More conclusions coming...

6 ACKNOWLEDGEMENTS

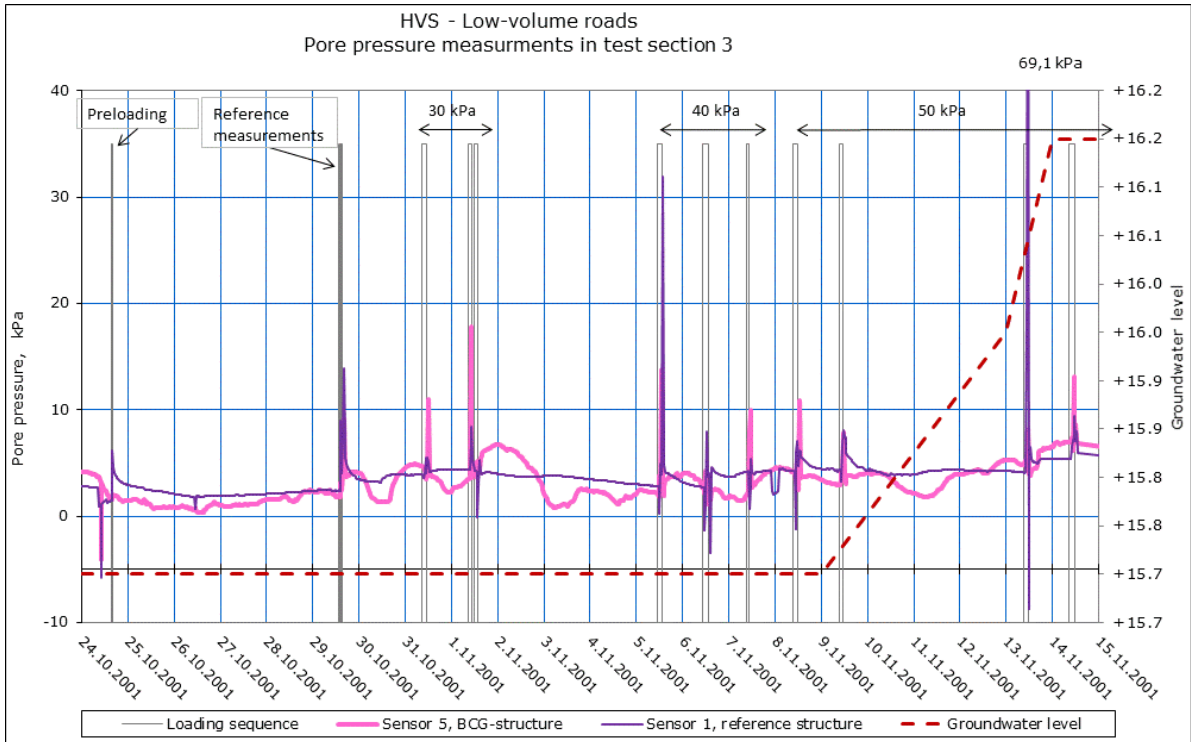


Figure 8. Measured pore pressures in test section 3 with 30, 40 and 50 kPa load sequences.

7 REFERENCES

- Bilodeau, J-P. & Doré, G. 2012. Water sensitivity of resilient modulus of compacted unbound granular materials used as pavement base, *International Journal of Pavement Engineering*, 13:5, 459-471, DOI: 10.1080/10298436.2011.573556
- Cedergren, H. R. 1994. "America's pavements: World's longest bathtubs." *Civil Eng.* 64(9), 56-58.
- Christopher, B. R., and McGuffey, V. C. (1997). NCHRP synthesis of highway practice 239: Pavement subsurface drainage systems, National Research Council, Washington, DC.
- Ho, X. N., Nowamooz, H., Chazallon, C., & Migault, B. 2014. Effect of hydraulic hysteresis on low-traffic pavement deflection, *Road Materials and Pavement Design*, 15:3, 642-658, DOI: 10.1080/14680629.2014.906364
- Korkiala-Tanttu, L., Jauhiainen, P., Halonen, P., Laaksonen, R., Juvankoski, M., Kangas, H. & Sikiö, J. 2003. Effect of steepness of sideslope on rutting. Research of low-volume roads, HVS-test structures. Finnra Reports 19/2003. Finnish Road Administration, Helsinki. 40 p. + 17 app.
- Korkiala-Tanttu, L., Rathmayer, H. & Kangas, H. 2002. Performance evaluation of a Bi-component geotextile in accelerated pavement test, The Seventh International Conference on Geosynthetics. Nice, France. 22-27. September, 2002. Geosynthetics - 7th ICG- Delmas. A.A. Balkema Publishers. Rotterdam, The Netherland (2002), 885-888
- Saevarsdottir, T. & Erlingsson, S. 2013. Effect of moisture content on pavement behaviour in a heavy vehicle simulator test, *Road Materials and Pavement Design*, 14:sup1, 274-286.